Title

Ca isotope fractionation in a high-alkalinity lake system: Mono Lake, California

Authors

Nielsen, Laura C

DePaolo, Donald J

Publication Date

2013-10-01

DOI

10.1016/j.gca.2013.05.007

Ca isotope fractionation in a high-alkalinity lake system: Mono Lake, California

Laura C. Nielsen[1*] & Donald J. DePaolo[1,2]

[1]Center for Isotope Geochemistry, University of California-Berkeley, Berkeley, CA, 94720

[2]Lawrence Berkeley National Laboratory, Berkeley, CA, 94720

*corresponding author: lnielsen@berkeley.edu

ABSTRACT

Precipitation of calcium carbonate minerals from aqueous solution induces surface-controlled kinetic stable Ca isotope fractionation, where the magnitude of fractionation depends on the relative rates of ion attachment to and detachment from the mineral surface. Changing solution stoichiometry or the Ca^{2+}:CO_3^{2-} activity ratio affects the mineral surface composition and may affect stable isotope fractionation during growth. No experimental studies have investigated the effects of varying solution stoichiometry on calcium isotope partitioning during calcite or aragonite growth, but natural alkaline lake systems such as Mono Lake, California provide a test bed for the hypothesized stoichiometry dependence. Mono Lake has a Ca^{2+}:CO_3^{2-} activity ratio of about 0.001, six orders of magnitude lower than ocean water and typical terrestrial freshwater. Our chemical and isotopic measurements of the major components of the calcium isotope budget of Mono Lake yield novel evidence of significant kinetic Ca isotope fractionation during calcite, aragonite and magnesian calcite precipitation from alkaline lake water. Streams and springs supply Ca to the lake, and a substantial proportion of this supply is precipitated along the lake shore to form tufa towers. Lake water is 30 × oversaturated with respect to calcite due to growth rate inhibition by orthophosphate, so $CaCO_3$ also precipitates directly from the water column to form carbonate-rich bottom sediments. The Sr isotopic composition is used to estimate the proportions of fresh and alkaline lake water from which each solid carbonate sample precipitated. Carbonate minerals that precipitated directly from lake water (low Ca^{2+}:CO_3^{2-}) experience relatively large Ca isotope fractionation during growth. Tufa and shoreline carbonates that precipitated from lake water with a significant fraction of spring water are considerably less fractionated. Overall, the behavior of the Mono Lake Ca isotope system is similar to that of the global oceans; the average $\delta^{44/40}$Ca of lake water is positive (+0.3). Archived water samples indicate that the lake $\delta^{44/40}$Ca varied by over 2 ‰ between 1995 and 2010. The most extreme excursions are toward higher $\delta^{44/40}$Ca, and are probably caused by carbonate precipitation events induced by breakdown of chemostratification.

1. INTRODUCTION

Advances in the measurement of stable isotope variations of cations such as Ca, Fe, and Mg (Johnson et al., 2004) provide novel perspectives on mineral formation processes relative to the isotopes of more commonly used elements like C, O, H, S, and N. Calcium plays a major role in biogenic and inorganic processes central to the global carbon cycle (Gussone et al., 2003; Chang et al., 2004; DePaolo, 2004; Fantle and DePaolo, 2005). Precipitation of calcium carbonate minerals from aqueous solutions produces about 0.0 ‰ to 2.3 ‰ fractionation of ^{44}Ca/^{40}Ca between solid and aqueous phase (i.e. Skulan and DePaolo, 1999; Gussone et al., 2003; Lemarchand et al., 2004; DePaolo, 2004; Tang et al., 2008; Reynard et al., 2011), with light calcium isotopes preferentially incorporated into the solid phase.

The origin of Ca isotope fractionation associated with carbonate mineral precipitation is still uncertain, although there is increasing evidence of kinetic control. Kinetic isotope fractionation can arise from the mass dependence of diffusive aqueous and lattice transport rates (Richter et al., 2006; Bourg and Sposito, 2007), and the mass dependence of reaction rate constants. Both processes should result in the light isotope being preferentially incorporated into the solid phase. Available evidence suggests that diffusive fractionation of ^{44}Ca/^{40}Ca is not likely to exceed about 0.5 ‰ (Bourg et al., 2010). Both biogenic and inorganic calcium carbonate precipitation typically occur far from chemical equilibrium, so transport and surface-controlled effects – those that occur during the attachment of ions to or detachment of ions from the crystal bulk at the mineral-aqueous interface – are likely to determine reaction rates (Morse and Arvidson, 2002) and probably control isotope separation (DePaolo, 2011; Nielsen et al., 2012). Surface-controlled kinetic effects are also discernible in O isotopes during calcite precipitation (Kim and O'Neil, 1997; Dietzel et al., 2009).

Experimental and field investigations of Ca isotope fractionation during calcium carbonate precipitation have largely focused on aqueous solutions with seawater-like compositions, where the calcium ion activity greatly exceeds the carbonate ion activity $a_{Ca^{2+}} >> a_{CO_3^{2-}}$, and near-neutral pH (Gussone et al., 2003, 2004; Lemarchand et al., 2004; Gussone et al., 2005; Böhm et al., 2006; Tang et al., 2008). In such solutions, mineral precipitation may be limited by carbonate ion delivery to the growing mineral, but it is unlikely that aqueous diffusive transport limits the delivery of Ca or affects the Ca isotope composition of the growing mineral. For this reason, it is likely that the observed Ca isotope fractionations are controlled by surface reaction kinetics (DePaolo, 2011). For aqueous solutions where $a_{Ca^{2+}} << a_{CO_3^{2-}}$, such as in alkaline lakes or CO_2-rich springs, it is possible that diffusive aqueous transport could be important and could mask surface reaction effects.

In situ atomic force microscope (AFM) observations of calcite precipitation reveal a significant solution stoichiometry dependence of calcite growth kinetics (Larsen et al., 2010). Kinetic isotope fractionation is also likely to be affected by solution stoichiometry (Nielsen et al., 2012). Although no experiments have explicitly demonstrated the dependence of the calcium isotope fractionation factor on $a_{Ca^{2+}}$:$a_{CO_3^{2-}}$, natural laboratories exist for which the stoichiometry dependence of calcium isotope partitioning may be tested. Precipitation of calcium carbonate from alkaline lakes, where mixing of calcium-rich springs and carbonate-rich lake water drives mineral precipitation, provides one such proving ground.

In this study, we measured the Ca isotopic composition of calcium carbonate precipitated from an alkaline lake. The primary objectives were to determine if there is evidence that solution stoichiometry affects isotope partitioning during carbonate formation from alkaline solutions, and to characterize Ca isotope fractionation in this environment. More generally, the alkaline lake environment is a microcosm of the global Ca cycle (cf. Rocha and DePaolo, 2000), but one that can be more fully characterized, so it presents an opportunity to test models for Ca isotope fractionation in the weathering cycle.

[Figure 1 about here.]

Mono Lake is a highly alkaline closed-basin lake east of the Sierra Nevada in eastern central California (Fig. 1). Freshwater and Ca are delivered to the lake by streams and springs. Evaporation concentrates the dissolved constituents leading to precipitation of abundant calcium carbonate, both in sediments at the lake bottom and near the shore where spring water enters (Russell, 1889; Cloud and LaJoie, 1980). In the near-shore environment, calcite, aragonite and magnesian calcite precipitate where the spring water mixes with the high-pH, high CO_3^{2-}(aq) lake water, producing tufa towers that grow upward from the lake bottom. The precipitation of tufa is believed to be primarily an inorganic process (Dunn, 1953), despite the abundance of organisms embedded in tufa (Scholl and Taft, 1964). Nevertheless, the role of organic matter in tufa formation has yet to be fully established. The modern lake maintains a high ($\Omega > 10$) oversaturation with respect to calcium carbonate (Bischoff et al., 1993), probably due to inhibition of carbonate precipitation by phosphate (soluble reactive phosphate (SRP) > 600 μM; Bischoff et al., 1993; Jellison et al., 1993b).

2. METHODS

2.1. Sampling

Samples of carbonate tufa and Mono Basin waters were collected during the summers of 2009 and 2010. GPS coordinates for collection locations were recorded at the time of sampling. For each water sample, pH, temperature and conductivity were measured with a Thermo Scientific Orion StarTM Series pH and conductivity meter. Conductivity measurements were field calibrated with a 1413 μS/cm conductivity standard, and pH 4, 7 and 10 NIST-traceable buffers were used to calibrate pH prior to each measurement, and the 2 standard deviation (s.d.) uncertainty on each measurement is 0.03 pH units. Analyses of lake water pH are likely to be somewhat inaccurate due to the large difference in junction potential between the lake water and calibration buffers. All water samples were filtered through a 0.2 μm mesh to remove particulates, acidified on-site, and stored in 250 mL Milipore Stericup polystyrene flasks. Acidification of high alkalinity samples caused the evolution of CO_2, but this should not alter the cation composition of the samples. Mono Lake water samples 9, 10, 11 and 12 were collected offshore at various depths using a deep-water sampler. A single Mono Lake water sample collected in 2010 was filtered, refrigerated and not acidified for alkalinity and anion analysis. All fluid samples collected for this study were stored at room temperature and analyzed within 6 months of collection.

Lake bottom sediment (LBS) samples 1 and 2 were collected via Ekman grab and coring, respectively. Sample LBS 3 was obtained from the top few centimeters of a shoreline push core. Dense lithoid tufa samples were chipped off of tufa towers either above the lake surface or shallowly submerged. These tufa towers formed when the lake level was considerably higher than today, likely during the Holocene (Whiticar and Suess, 1998). No actively precipitating towers were observed at the time of sampling.

Archived lake and spring water samples were also obtained. These samples were stored at room temperature in sealed LDPE (lake water) or glass (spring water) containers to limit evaporation, and were only analyzed for Ca and Sr concentrations and isotopes. Spring waters were stored for no more than 9 years, and lake waters were stored up to 15 years. Archived samples were acidified in their original containers prior to analysis to ensure that any secondary phases formed since collection were incorporated into the sample aliquot.

2.2. Geochemical calculations

To evaluate the driving forces for carbonate precipitation, equilibrium speciation of lake and spring water was calculated using CrunchFlow 2007 (Steefel, 2009). This code uses an extended Debye-Hückel formulation to calculate the activity coefficients for aqueous species including Ca^{2+} and CO_3^{2-}. The original thermodynamic database does not contain magnesian calcite, a major constituent of tufa precipitated at Mono Lake. High (15 mol% Mg) and low (7 mol% Mg) magnesian calcite ($Mg_xCa_{1-x}CO_3$) were added to the database to account for these phases. The mol% $MgCO_3$ in Mono Lakes high magnesium calcite was previously determined to be 17% (Scholl and Taft, 1964), which is close to the value chosen for entry into the thermodynamic database. The form of high- and low- magnesian calcite precipitation reactions incorporated in the database is as follows:

$$xMg^{2+} + (1-x)Ca^{2+} + CO_3^{2-} \rightarrow Mg_xCa_{1-x}CO_3. \tag{2.1}$$

Magnesian calcite ion activity product (IAP) values were taken from Bertram et al. (1991), where the product is expressed as:

$$IAP = a_{Ca^{2+}}^{1-x} a_{Mg^{2+}}^{x} a_{CO_3^{2-}}. \tag{2.2}$$

The a values represent ionic activities, and x represents the mole fraction of Mg^{2+} incorporated into the solid. Stoichiometry and IAP values for high-Mg and low-Mg calcite reactions at 25°C included in the database are presented in Table 1 (Bischoff et al., 1987; Bertram et al., 1991). The molar volume of magnesian calcite was assumed to be the same as that of calcite, 36.9 cm^3/mol.

Thermodynamic driving force for mineralization is reported as the saturation index (SI = log(IAP/K_{sp})), where K_{sp} is the mineral solubility product. Speciation calculations predict supersaturation with respect to dolomite, but no dolomite is observed, probably because of kinetic limitations to significant Mg incorporation and dolomite precipitation (cf. Morse et al., 2007).

[Table 1 about here.]

2.3. Isotopic analyses

Calcium and strontium concentrations and isotope compositions were measured via the double-spike method at the Center for Isotope Geochemistry, University of California-Berkeley. Solid tufa and crust samples were dissolved in 3N HNO_3 and alkaline lake waters were reacted with 3N HNO_3 prior to spiking with a ^{42}Ca-^{48}Ca double spike for calcium, and an ^{84}Sr tracer for strontium. Freshwaters were spiked directly. Lake bottom sediment was rinsed with 18 MΩ doubly deionized (DI) water, centrifuged, and leached with acetic acid to extract calcium and strontium from the carbonate fraction. Acetic acid leaches are commonly used to extract the carbonate mineral fraction from sediments (i.e. Fantle and DePaolo, 2006). The leached sample was spiked and processed with tufa and water samples. Non-reactive residual phases including quartz, muscovite, and albite were determined using x-ray diffraction (Table 2). These are typical components of basement rock found in Mono Basin.

[Table 2 about here.]

Ca separation was performed using Ca-specific Eichrom DGA resin (Horwitz et al., 2005) on acid-washed Teflon columns with a resin volume of 250-300 μL and a reservoir volume of 1 mL. The DGA resin was suspended in DI water, and approximately 250 μL were pipetted into each column. The columns were rinsed thee times with 1 mL of DI water, once with 1 mL of 3N HNO_3 and once with DI water followed by a final 0.5 mL rinse with 3N HNO_3. Spiked samples were dried and redissolved in 100 μL 3N HNO_3, which was pipetted directly onto the clean resin. Loaded columns were then sequentially rinsed with 100, 300 and 500 μL of 3N HNO_3. Calcium was collected using a final rinse of 1 mL DI water.

Approximately 3 μg of spiked and separated calcium was loaded with 20 $\%$ H_3PO_4 onto zone-refined Re double filaments and loaded into a Finnigan Triton multicollector thermal ionization mass spectrometer (TIMS) for analysis. For details on the analytical procedure see Nielsen et al. (2011). Calcium isotopic compositions are reported in the standard delta notation (‰) relative to bulk silicate Earth (BSE), with ^{44}Ca/^{40}Ca = 0.0212094(3) (Simon and DePaolo, 2010):

$$\delta^{44/40}Ca = \left(\frac{([^{44}Ca]/[^{40}Ca])_{sample}}{([^{44}Ca]/[^{40}Ca])_{BSE}} - 1 \right) \times 1000. \tag{2.3}$$

NIST SRM 915a is used as a laboratory standard and has a $\delta^{44/40}$Ca of -0.97(04) relative to BSE (Simon and DePaolo, 2010). This standard is no longer available and has been replaced by NIST SRM 915b (-0.25(04) relative to BSE; Heuser and Eisenhauer, 2008). The external reproducibility (2 s.d.) associated with all $\delta^{44/40}$Ca measurements is 0.15. Each reported $\delta^{44/40}$Ca is the average of at least two replicate analyses. Isotope dilution measurements of calcium concentration yield uncertainties of within 2 % relative standard deviation (RSD).

Sr isotope separations were performed on cation exchange columns using Eichrom Sr Spec resin. Separation and measurement details may be found in Fantle and DePaolo (2006). ^{87}Sr/^{86}Sr ratios are reported with 2 s.d. internal errors, and uncertainties on Sr isotope dilution concentration measurements have been estimated to be within 2 %RSD. The composition and reproducibility of the NBS 987 laboratory Sr standard using this method is 0.71024(1) (2 s.d.). Errors are reported for individual measurements where they exceed the external reproducibility of the standard.

2.4. Major and trace element concentrations

Trace metal concentrations were measured on water samples by ICP-MS at the Lawrence Berkeley National Laboratory. Before analysis, samples were acidified to 2% by volume HNO_3 using ultra high purity (BDH Aristar Seastar) nitric acid diluted with 18.3 MΩ high purity water. Samples were then spiked with internal standards. Samples were then analyzed on a PerkinElmer Elan DRCII ICP-MS using a multi-element method with ^{6}Li, ^{71}Ga, ^{115}In, ^{169}Tm and ^{193}Ir as internal standards. To eliminate interferences, K and Ca were analyzed with NH_3 as a reaction gas. NIST SRM 1643e was used to validate the method. Reproducibility of analyses is better than ± 5 %RSD, and all measured species were well above instrumental detection limits.

Total dissolved inorganic carbon (DIC) was measured using a Shimadzu TOC-V$_{CSH}$. Fluid samples were injected into the IC reaction vessel containing a continually sparged phosphoric acid solution. Volatilized CO_2 was measured by a non-dispersive infrared gas analyzer (NDIR) using TOC-Control V software. Anions were analyzed using a Dionex ICS-2100 with AS-DV autosampler and KOH (potassium hydroxide) eluent. Sample fluid was injected into the column and analyzed using Chromeleon 7 software. Both DIC and anion analyses have a 0.05 ppm detection limit, and an RSD of 2 %.

3. RESULTS

[Table 3 about here.]

3.1. Sr and Ca isotopic compositions

Our objective was to evaluate the Ca isotopic fractionation associated with aragonite and calcite precipitation from Mono Lake water, and to constrain the calcium budget of Mono Basin in the recent past. The lake is a dynamic system with water and dissolved constituents continuously being added from streams and springs. Carbonate minerals can be precipitated from mixed lake and freshwaters, so it is necessary to have a tracer that can provide information on the components of the waters from which they precipitate. We used Sr isotopes for this purpose, because there is substantial variability in the Sr isotopic composition of water inputs to the lake. The Sr and Ca isotopic composition of lake, stream, spring, tufa, crust and lake bottom sediment samples from the Mono Basin are shown in Table 3. Sample locations corresponding to Ca isotopic results are shown in Fig. 1. Isotopic data are plotted in Figs. 2 and 7.

[Figure 2 about here.]

3.1.1. Compositions of stream waters

Stream waters flowing from the Sierra Nevada constitute the main flux of water and chemical constituents to the lake (Garrels and Mackenzie, 1967) and have ^{87}Sr/^{86}Sr values between 0.70882 and 0.71153. The observed variability in Sr isotope ratios reflects the range of values measured in Mono Basin bedrock (Neumann and Dreiss, 1995). The two largest streams flowing into Mono Lake, Rush Creek (Neumann and Dreiss, 1995) and Lee Vining Creek, have a narrower range of isotopic values; ^{87}Sr/^{86}Sr of 0.70971 and 0.70976, and $\delta^{44/40}$Ca of -0.83 and -0.68 respectively. The average $\delta^{44/40}$Ca of streams flowing into Mono Lake from the Sierra Nevada is -0.77(13) (2 s.d., n = 4).

The variability of the ^{87}Sr/^{86}Sr in Sierran stream waters may be explained by selective mineral weathering of source rocks (e.g. Blum et al., 1993; Neumann and Dreiss, 1995) as well as by lithologic heterogeneity in the stream drainage basins. Each stream samples a distinct subset of intrusive rocks with different Rb/Sr and initial ^{87}Sr/^{86}Sr ratios as well as different proportions of metamorphic roof pendant rocks. Roof pendant rocks vary widely in proportion of siliceous and carbonate components and are generally early Paleozoic in age. There is evidence that prior to 300 Ma, seawater (and limestone) had $\delta^{44/40}$Ca about 0.5 ‰ lower than today (Farkaš et al., 2007), which is consistent with observed light stream water $\delta^{44/40}$Ca values.

3.1.2. Compositions of spring waters

High-Ca spring water samples ($>$ 4 ppm) span a wide range of strontium isotopic compositions (0.70646-0.70976), similar in magnitude to stream water variability and well within the range reported by Neumann and Dreiss (1995). These springs are associated with low ^{44}Ca/^{40}Ca (-0.38 to -0.83). The majority of Ca entering the lake by way of springs is likely sourced by the same lithologies as stream water and is therefore similar in Sr and Ca isotopic composition.

Low-calcium spring water sampled directly adjacent to tufa towers along the northern shore (Fig. 2 and 7) has an average ^{87}Sr/^{86}Sr value of 0.7083(4), which falls within the range of non-western-shoreline spring Sr isotopic compositions presented by Neumann and Dreiss (1995). Springs represent the low-^{87}Sr/^{86}Sr groundwater typical of the areas dominated by Miocene and younger volcanic rocks (Neumann and Dreiss, 1995). The $\delta^{44/40}$Ca of low-Ca ($<$ 2.1 ppm) springs are between 0.34 and 0.78. The high $\delta^{44/40}$Ca may result from precipitation of isotopically light calcium-bearing minerals *en route* to the surface. Ca-depleted spring waters are not thought to contribute significantly to tufa formation.

3.1.3. Composition of Mono Lake water

Mono Lake water is spatially variable in both Ca and Sr isotopic composition. The ^{87}Sr/^{86}Sr of the lake falls between 0.7089(1) and 0.70916(6), and $\delta^{44/40}$Ca of lake water sampled on a single day varies from 0.16 to 0.60. The average $\delta^{44/40}$Ca of 2009 Mono Lake water was 0.34(14) (1 s.d., n = 10) and the average ^{87}Sr/^{86}Sr is 0.7091(2).

The concentration and calcium isotopic composition of Mono Lake water changes dramatically with time (Figs. 6 and 4), while the strontium isotopic composition remains nearly invariant, despite the short residence time of both (5-25 yr and $\sim$ 20 yr respectively).

Between 1950 and the mid-1990s, most reported lake water calcium concentrations are approximately 4 ± 2 ppm (EIR, 1993; Bischoff et al., 1993; Jellison et al., 1993a; Neumann and Dreiss, 1995), so we infer that this concentration represents the long term average lake water calcium concentration. Between 1996 and 2010, the calcium concentration has varied between 2.5 and 12.5 ppm, indicating variability in the lake water calcium budget. Concentration is strongly correlated with $\delta^{44/40}$Ca in lake water; calcium-rich (12.5 ppm) lake water is light (-0.17), while calcium-poor (2.5 ppm) lake water is extremely heavy (2.14). The rapid changes in calcium isotope composition are expected considering the short (5-25 yr) residence time of calcium in Mono Lake. The isotopic composition of 4 ppm Mono Lake water – $\delta^{44/40}$Ca = 0.80 – likely reflects the long term average composition of the lake.

3.1.4. Compositions of precipitated carbonate minerals

Tufa sampled from the northern lake shore falls within a narrow range of ^{87}Sr/^{86}Sr, 0.70891-70902 (Table 3). The average ^{87}Sr/^{86}Sr of calcium-depleted shoreline springs located adjacent to sampled tufa, 0.7083(4), is lower than tufa, 0.7090(3), with a probability (p) of the null hypothesis equal to 3e-6 from the two-sample equal variance student's t test. The average ^{87}Sr/^{86}Sr of Mono Lake water is higher than tufa, and this difference is also statistically significant ($p = 0.01$). The tufa Sr isotopic composition is a measure of the proportions of water from different sources. Assuming a reasonably constant Mono Lake water Sr isotopic composition, the measured ranges and values indicate that the Sr isotopic composition of tufa is controlled primarily by Mono Lake water, but with a minor spring water contribution.

The $\delta^{44/40}$Ca values of tufa towers sampled in this study are between -0.73 and -0.40. The calcium isotopic composition of tufa collected from Navy Beach along the southern lake shore (Tufa 11; $\delta^{44/40}$Ca = -0.64) is identical in $\delta^{44/40}$Ca to the average calcium isotopic composition of northern tufa, -0.62(21) ($n = 8$, 2 s.d.). Tufa samples were crushed and homogenized prior to analysis, so each represents the composition averaged over many years of growth. Sampled tufa towers likely formed at different times, so the minimal isotopic variability suggests that the long-term Mono Lake Ca isotope budget is reasonably constant.

Recently precipitated salt crusts coat the northern shoreline of Mono Lake. These crusts are likely formed due to evaporation of lake water accompanied by mixing with spring water. Sodium carbonate and chloride minerals including trona and halite make up the bulk of these crusts. Minor carbonate minerals present in the crusts have $\delta^{44/40}$Ca values of -0.7 and -0.57, in the middle of the range found for tufa (Table 3). The ^{87}Sr/^{86}Sr ratios of the crust carbonate are substantially lower than those of tufa, which indicates that the water from which they precipitated had a significant proportion of low-^{87}Sr/^{86}Sr spring water.

The $\delta^{44/40}$Ca of contemporary lake bottom sediment collected far from shore varied from -0.39 to -0.30 (Fig. 2). A single sample of down-core sediment has a significantly lower $\delta^{44/40}$Ca = -0.94, indicating that the lake bottom sediments may reflect recent changes to the lake water isotopic composition. The lake bottom sediment carbonate mineral fraction precipitates directly from the water column and is therefore not affected by mixing with spring waters along the shoreline. Lake bottom carbonate is a significant component of the Mono Basin Ca budget.

4. DISCUSSION

4.1. Mono Lake Ca isotope budget

The Ca budget of Mono Lake is schematically portrayed in Fig. 3. Most calcium enters the basin via streams from the Sierra Nevada (EIR, 1993; Tomascak et al., 2003), which contain dissolved mineral weathering products (e.g. Garrels and Mackenzie, 1967). Silicate mineral weathering is supplemented by the dissolution of small amounts of secondary calcium carbonate and marble during water transport to the lake. Water flowing from the Sierra Nevada constitutes the greatest influx of Ca to Mono Lake (denoted F_{SN}), so the Ca isotopic composition of Sierra streams and springs is approximately equal to the isotopic composition of the Ca supply to the lake. A recent estimate of the total Ca flux to Mono

Lake is 2.21×10^6 kg Ca/yr, with contributions from streams (1.75×10^6 kg Ca/yr), groundwater (4.5×10^5 kg Ca/yr), and springs (1.25×10^4 kg Ca/yr; Tomascak et al., 2003). The total stream runoff corresponding to these Ca fluxes as reported by Tomascak et al. (2003) is close to the total average tributary inflow based on an assessment of stream runoff entering Mono Lake between 1940 and 1989 (1.532×10^{11} L/yr) (EIR, 1993).

[Figure 3 about here.]

Precipitation of carbonate minerals is the primary mode of calcium removal from the lake. The flux of Ca into carbonate minerals at the shoreline (into tufa) is denoted by F_{Tf}, while the flux of Ca from the water column to sediments on the modern lake bottom as aragonite and calcite particles is denoted by F_{cs}. Inorganic $CaCO_3$ makes up $\sim 4\ \%$ of the lake bottom sediment fraction, and sediment accumulates at an average rate of 0.59 kg m^{-2} yr^{-1} (Li, 1995). Using the current lake area of $\sim 1.8\times10^8$ m^2, the rate of Ca sedimentation at the lake bottom is $F_{cs} = 1.72\times10^6$ kg Ca/yr. When the lake is at steady state with respect to calcium supply and removal ($F_{SN} = F_{cs} + F_{Tf}$), tufa precipitation must account for $\sim 22\ \%$ of the Ca flux from Mono Lake. This value is presumably an upper limit, because the lake area was significantly larger than its current size throughout most of the Holocene.

We use isotopic mass balance to model the calcium isotope variability of Mono Lake water between 1996 and 2010 following DePaolo (2004). No isotopic data are available for Mono Lake water preceding 1996, so we did not attempt to reconstruct the Mono Basin calcium budget prior to this date. The rate of change of $\delta^{44/40}Ca_{Lk}$ can be written as:

$$N_{Ca}\frac{d\delta^{44/40}Ca_{Lk}}{dt} = F_{SN}(\delta^{44/40}Ca_{SN} - \delta^{44/40}Ca_{Lk}) - F_{Tf}\Delta^{44/40}Ca_{Tf} - F_{cs}\Delta^{44/40}Ca_{cs}, \tag{4.1}$$

where N_{Ca} is the total moles of calcium in Mono Lake, and $\delta^{44/40}Ca_{Lk}$ and $\delta^{44/40}Ca_{SN}$ represent the calcium isotopic compositions of of Mono Lake water and Sierra Nevada stream water. Isotopic fractionation between tufa and lake water and between carbonate sediment and lake water are defined: $\Delta^{44/40}Ca_{Tf} = \delta^{44/40}Ca_{Tf} - \delta^{44/40}Ca_{Lk}$, and $\Delta^{44/40}Ca_{cs} =$

$\delta^{44/40}$Ca$_{cs}$ - $\delta^{44/40}$Ca$_{Lk}$. Precipitation of carbonate minerals in shoreline crusts ($\Delta^{44/40}$Ca$_{cr}$ = $\delta^{44/40}$Ca$_{cr}$ - $\delta^{44/40}$Ca$_{Lk}$) probably does not contribute significantly to the Ca budget of the lake. The variability of lake volume (LADWP, 2010) and concentration are known, so N$_{Ca}$ may be determined as a function of time. For simplicity, the carbonate precipitation flux terms (F$_{Tf}\Delta^{44/40}Ca_{Tf}$ - F$_{cs}\Delta^{44/40}Ca_{cs}$) have been grouped into a single term (F$_{C}\Delta^{44/40}Ca_{C}$). The magnitude of the fractionation factor due to precipitation was assumed to be constant and representative of average carbonate mineral growth.

We modeled the recent calcium budget for Mono Lake by accounting for observed changes in lake water volume and calcium concentration (Fig. 4). To calculate the rate of change in calcium isotopic composition in a given year, calcium fluxes to and from the lake must be determined (Eq. 4.1). Assuming stream flow and evaporation constitute the primary fluxes of water to Mono Lake, the flux of stream water to the lake (F$_s$) may be determined from the expression,

$$\frac{dV}{dt} = F_s - F_{EV}, \tag{4.2}$$

where F$_{EV}$ is the evaporative flux of water from the lake. The basin is assumed to maintain a constant F$_{EV}$ of 1.7×10^{11} L/yr, which equates to 1.2 m of evaporation from the lake annually at its current volume. Estimates of evaporative flux from the lake range between 0.89 - 1.2 m/yr (EIR, 1993). The fluxes of calcium to (F$_{SN}$) and from (F$_C$) the lake may be calculated from,

$$\frac{dN_{Ca}}{dt} = F_s c_s - F_C, \tag{4.3}$$

where c$_s$ is the average concentration of calcium in stream water ($\sim$ 10 ppm; Tomascak et al., 2003) and F$_{SN}$ = F$_s$c$_s$. We assume $\frac{dN_{Ca}}{dt}$ to be constant within each interval. The budget was optimized using a $\Delta^{44/40}$Ca$_C$ value of -1.2 ‰ and a $\delta^{44/40}$Ca$_{SN}$ of -0.20. The fitted $\delta^{44/40}$Ca$_{SN}$ is somewhat higher than the calcium isotopic compositions of stream water reported in this study (Table 3), but it is considered reasonable given the simplicity of this model.

Between 2004 and 2005, the concentration of Ca in the lake abruptly plummeted. This distinctive event and the corresponding increase in $\delta^{44/40}\mathrm{Ca}_{Lk}$ may be explained by an abrupt carbonate mineral precipitation event. A rapid precipitation event occurring around 2004 is consistent with the breakdown of meromixis – persistent chemostratification of lake water – in 2003. Prior to 2003, the lake had not mixed since 1995 (Jellison and Roll, 2003), before our Ca isotope record begins. Presumably the calcium concentration of shallow lake water increased gradually between 1995 and 2003, but we do not have sufficient temporal resolution in our sample record to validate this. Breakdown of meromixis can promote a rapid precipitation event by mixing Ca-rich surface waters with Ca-depleted alkaline bottom waters and has been invoked to explain $CaCO_3$-rich horizons in lake bottom sediment (Newton, 1994). This explanation is consistent with the lack of variability in ^{87}Sr/^{87}Sr during this period. Rapid changes in the input fluxes to the lake would change both $\delta^{44/40}$Ca and ^{87}Sr/^{87}Sr, while a precipitation event would only affect $\delta^{44/40}$Ca.

In the absence of major stream flow variability or the onset of meromixis, the lake water should return to a steady state composition within $\sim$10 years, the current residence time of calcium in the lake. The simple budget presented here confirms that carbonate minerals precipitated in Mono Basin are isotopically lighter than their source fluids. A thorough analysis of the driver for $CaCO_3$ precipitation is needed to more precisely quantify this offset and its underlying cause.

[Figure 4 about here.]

4.2. Geochemistry of carbonate precipitation

4.2.1. Phosphate inhibition and growth rate

[Table 4 about here.]

In this section, we employ thermodynamic and kinetic calculations to investigate the driving force for carbonate mineralization in Mono Basin. Our x-ray diffraction data from solid tufa samples and shoreline crusts reveal that tufa is primarily composed of aragonite, with lesser amounts of high- and low- magnesian calcite (Table 2). Calculated saturation indices of minerals in mixed spring and lake water end-member solutions (Table 4) demonstrate that the saturation index (SI) of all tufa $CaCO_3$ decreases monotonically with the fraction of freshwater added to the lake water, even when Ca-rich waters enter the lake (Fig. 5). The addition of Ca-rich groundwater apparently does not promote tufa precipitation, because the process does not increase SI. Based on the abundant tufa located along the lakeshore, it is clear that spring water mixing facilitates $CaCO_3$ precipitation in some way, so the distribution of carbonate minerals must be kinetically controlled.

[Figure 5 about here.]

Orthophosphate is known to inhibit the precipitation of calcium carbonate minerals by forming inner-sphere complexes on actively precipitating surface sites (e.g. kinks) of nascent calcium carbonate nuclei and of growing layers (Dove and Hochella, 1993; Lin and Singer, 2006). The preservation of high lake water carbonate mineral supersaturation has been attributed to the high concentration of orthophosphate in Mono Lake ($\sim$60 ppm Bischoff et al., 1993). However, the effect of the changing orthophosphate concentrations associated with mixing between lake and spring water has not previously been considered. In the remainder of this section we evaluate the role of orthophosphate in tufa formation.

Burton and Walter (1990) derived an empirical relationship between phosphate concentration and speciation and calcium carbonate precipitation rate from seawater. For aragonite,

$$log(R_p) = -6.96 - 1.19log([PO_4^{3-}]) + 1.63log(\Omega_a - 1), \tag{4.4}$$

Where R_p is precipitation rate in units of μmol m^{-2} h^{-1}, brackets denote aqueous concentration (mol/kg), and Ω_a is oversaturation with respect to aragonite, $10^{SI_{aragonite}}$. For calcite, the expression is:

$$log(R_p) = -6.50 - 1.18log(0.85[PO_4^{3-}] + 0.15[HPO_4^{2-}]) + 1.90log(\Omega_c - 1), \tag{4.5}$$

where Ω_c is oversaturation with respect to calcite, $10^{SI_{calcite}}$. For our analysis, we use concentrations and water temperatures based on Bischoff et al. (1993), and account for the temperature difference of 5° versus 15°C between typical lake water and spring water, respectively.

The precipitation rates of aragonite and magnesian calcite calculated from Eqs. 3 and 4 are shown in Fig. 5 plotted against the fraction of lake water in a mixture of lake and spring water. The maximum aragonite precipitation rate is obtained for mixtures with 98$\%$ lake water. The calculated calcite precipitation rate is highest for pure lake water and decreases markedly with the addition of spring water. This calculation shows clearly that aragonite is the preferred precipitate, which is consistent with the predominance of aragonite in tufa. In pure lake water, however, the calculation predicts that both calcite and aragonite should precipitate at reasonable rates. This latter result suggests that carbonate in the lake bottom sediment should have a larger proportion of calcite relative to aragonite in comparison with tufa. The carbonate mineralogy of Holocene lake bottom sediments deposited at water depths greater than 7 m is predominantly calcite, whereas aragonite dominates the carbonate fraction of shallow water core samples (Newton, 1994).

Precipitation kinetics are controlled by elementary ion attachment and detachment reactions at the mineral aqueous interface, and these same reactions control isotopic composition (e.g. Nielsen et al., 2012). In the following section, we consider the effects of mixed growth solution composition on $\Delta^{44/40}$Ca.

4.2.2. Mixing and Fractionation

[Table 5 about here.]

[Figure 6 about here.]

[Table 6 about here.]

To obtain a refined estimate of the Ca isotopic fractionation associated with the formation of tufa, we use the ^{87}Sr/^{86}Sr of each carbonate mineral sample to estimate the fraction of spring water present in the water from which it precipitated, and then calculate the $\delta^{44/40}$Ca of the mixed water. End-member spring and lake water Sr and Ca compositions used in the isotopic budget are listed in Table 5.

The calcium isotopic composition of a calcium-rich spring, Tufa spring, was used as the end-member spring $\delta^{44/40}$Ca = -0.80 (Table 3). The calcium isotopic composition of Tufa spring is similar to Sierra Nevada stream water, so it likely represents the primary Ca composition entering the lake. The ^{87}Sr/^{86}Sr representative of northern springs adjacent to sampled tufa, 0.7083(4), was used as the end-member spring strontium isotopic composition. Since tufa and crusts are localized precipitates, their Sr isotopic composition should only be affected by nearby spring and lake water, which directly supply the Ca and Sr involved in growth. The end-member lake water calcium isotopic composition is equal to the lake water isotopic composition of long term average (4 ppm) lake water, with $\delta^{44/40}$Ca = 0.80, and the end-member lake strontium isotope composition is equal to the current lake water average value of 0.7091(2)). We calculate the isotopic compositions of water mixtures from:

$$\delta_{tufa} = \frac{x_{spr}C_{spr}\delta_{spr} + (1 - x_{spr})C_{Lk}\delta_{Lk}}{x_{spr}C_{spr} + (1 - x_{spr})C_{Lk}}. \tag{4.6}$$

In this equation, C is concentration, δ is the isotopic composition (^{87}Sr/^{86}Sr or $\delta^{44/40}$Ca), and x$_{spr}$ is the mass fraction of spring water in the mixture. A mixing line based on solutions of Eq. 4.6 for Sr and Ca is depicted as a dashed line in Fig. 7. The $\delta^{44/40}$Ca value of the water from which the calcium carbonate samples precipitated is estimated from the value given by this line for the ^{87}Sr/^{86}Sr value of the sample. Fraction of lake water may also be calculated using this mixing relationship (Table 6). In general, the water mixtures have slightly lower $\delta^{44/40}$Ca than lake water. We cannot verify the composition of mixed or end-member fluids present at the time of carbonate formation, so our estimates of mixing and fractionation must be considered as approximations.

[Figure 7 about here.]

Calculated fractionation factors associated with tufa precipitation from mixed lake and spring water are presented in Table 6. The calcium isotopic composition of end-member lake water has a large influence on the calculated fractionation factor, so calculated $\Delta^{44/40}$Ca values for tufa, crust and lake bottom sediment for alternate $\delta^{44/40}\mathrm{Ca}_{Lk}$ are also given (Table 6). Although we believe the 2005 lake water calcium isotopic composition ($\delta^{44/40}\mathrm{Ca}_{Lk}$ = 0.80) likely reflects the long term average value, alternate $\Delta^{44/40}$Ca values are presented to demonstrate the possible range of values. These were calculated based on the average 2009 (0.34(14)) and the 1996 (2.14) $\delta^{44/40}\mathrm{Ca}_{Lk}$ values .

The calculated range of fractionation factors for precipitated tufa is $\Delta^{44/40}\mathrm{Ca}_{Tf}$ = -0.6 to -1.1 ‰. Shoreline crusts are fractionated by $\Delta^{44/40}\mathrm{Ca}_{cr} \sim$ -0.1 to -0.4 ‰ relative to mixtures of lake and spring water. Aragonite in intermediate depth (15 m) lake bottom sediment (LBS 1) is 1.1 ‰ lighter than long term average lake water, and the presence of a purely aragonitic sediment fraction is consistent with the sediment mineralogy reported by Li (1995). Calcite and aragonite from a deeper-water (36 m depth) lake bottom sediment sample (LBS 2) were slightly more fractionated than LBS 1 ($\Delta^{44/40}\mathrm{Ca}_{cs}$ = -1.2 ‰). The calculated fractionation factors are similar in magnitude to those found for both inorganic and biogenic calcium carbonate precipitation in natural and experimental settings (Gussone et al., 2003; DePaolo, 2004; Lemarchand et al., 2004; Gussone et al., 2005; Tang et al., 2008). Despite the fact that lake bottom sediment carbonates contain a greater proportion of calcite compared with the primarily aragonitic tufa towers (Table 2), they are more strongly fractionated than tufa or shoreline crusts. Aragonite is isotopically lighter than calcite when precipitated under similar conditions (Gussone et al., 2005), so mineralogy apparently does not control calcium isotope fractionation in this system.

Ikaite precipitation has been observed during the winter months at Mono Lake, and it has been hypothesized that tufa are formed in part by an ikaite precursor (Bischoff et al., 1993; Whiticar and Suess, 1998). Calcium isotope fractionation between ikaite and aqueous solution is smaller than for either calcite or aragonite, up to $\Delta^{44/40}\mathrm{Ca} \sim$ -0.7 ‰ (Gussone et al., 2011). It is possible that ikaite precipitation contributed in part to the calcium isotopic composition of tufa, but ikaite deposits are delicate and ephemeral, easily dispersed by waves and unstable for much of the year. It is likely that thinolitic tufa (calcite pseudomorphs) were formed by ikaite transformation (Whiticar and Suess, 1998), but no thinolitic tufa was analyzed in this study. Given the dearth of evidence supporting ikaite transformation to dense lithoid tufa, we do not explore this potential mechanism further here.

4.2.3. Solution stoichiometry dependence of tufa fractionation

Currently, all previously reported Ca isotope fractionation between carbonate minerals and aqueous solution involve precipitation under conditions where $a_{Ca^{2+}} >> a_{CO_3^{2-}}$. Mono Lake is different in that $a_{Ca^{2+}} << a_{CO_3^{2-}}$. The kinetics of calcite precipitation are strongly affected by $a_{Ca^{2+}}$:$a_{CO_3^{2-}}$ (Larsen et al., 2010), so it might be expected that Ca isotope fractionation could also depend on solution stoichiometry. The calcium to carbonate ratio could affect kinetic isotope fractionation in two ways: (1) through mass dependent rates of ion transfer to the mineral surface, and (2) through mass dependent ion attachment and detachment reactions with the mineral bulk. In this section we evaluate the potential effects of these mechanisms on the isotopic compositions of precipitated carbonate minerals.

Transport control alone is easily ruled out based on the observed magnitudes of $\Delta^{44/40}$Ca$_C$. If diffusive transport of Ca in solution were rate-limiting for calcite or aragonite growth, $\Delta^{44/40}$Ca$_C$ would not be expected to exceed ~-0.45 ‰, the magnitude of Ca^{2+} ion diffusive isotope separation (Bourg et al., 2010). Because the calculated fractionation factor of most carbonate minerals reported in this study significantly exceeds this threshold value, we propose that the observed kinetic isotope fractionation is primarily controlled by the kinetics of ion attachment and detachment at the mineral surface.

Mono Basin carbonate mineral $\Delta^{44/40}$Ca and associated growth solution stoichiometry calculated from the mixing of spring and lake water endmembers is plotted in Fig. 8. Carbonate crusts grown from solutions with a large proportion of spring water, and a correspondingly high $a_{Ca^{2+}}$:$a_{CO_3^{2-}}$, have smaller fractionation factors. Lake bottom sediments precipitated from pure lake water with a very low $a_{Ca^{2+}}$:$a_{CO_3^{2-}}$ have the largest fractionation factors observed in this study. Tufa samples span a large intermediate range of lake-spring water mixing proportions, and these are consistent with a decreasing fractionation factor with increasing proportion of low ^{87}Sr/^{86}Sr spring water. The qualitative relationship between solution stoichiometry and isotopic fractionation is consistent with the hypothesis that low $a_{Ca^{2+}}$:$a_{CO_3^{2-}}$ may inhibit isotopic equilibration between the growing mineral surface and solution (Nielsen et al., 2012).

[Figure 8 about here.]

Nielsen et al. (2012) presented a model for solution composition-dependent Ca isotope fractionation during calcite precipitation, which accounts for the effects of both supersaturation and solution stoichiometry on $\Delta^{44/40}$Ca. Assuming ion i (Ca^{2+} or CO$_3^{2-}$) with solution activity a_i attaches to the mineral surface at kink sites with attachment frequency k$_i a_i$ (s^{-1}) and detachment frequency ν_i (s^{-1}), growth rate may be expressed in terms of the activities of Ca^{2+} and CO$_3^{2-}$ in solution and elementary coefficients of attachment and detachment k$_i$ and ν_i (Nielsen et al., 2012). The net isotopic fractionation factor α_p – the calcium isotopic fractionation factor during precipitation – may be expressed:

$$\alpha_p = \frac{\alpha_f k_{Ca^{2+}} a_{Ca^{2+}} P_{CO_3^{2-}}}{k_{Ca^{2+}} a_{Ca^{2+}} P_{CO_3^{2-}} + \nu_{Ca^{2+}} P_{Ca^{2+}} (\frac{\alpha_f}{\alpha_{eq}} - 1)} \tag{4.7}$$

where α_f is the kinetic end-member fractionation factor, α_{eq} is the equilibrium calcium isotope fractionation factor between CaCO$_3$ and solution, P$_{Ca}$ is the probability that a given kink site is occupied by calcium, and P$_{CO_3}$ is the probability that a kink site is occupied by carbonate. Fractionation factor α_p is equivalent to the ratio of ^{44}Ca/^{40}Ca in the solid divided by the ratio of ^{44}Ca/^{40}Ca in the fluid. Kink site probabilities may be expressed in terms of elementary exchange coefficients and the activities of calcium and carbonate in solution:

$$P_{Ca^{2+}} = \frac{k_{Ca^{2+}} a_{Ca^{2+}} + \nu_{CO_3^{2-}}}{k_{Ca^{2+}} a_{Ca^{2+}} + \nu_{CO_3^{2-}} + k_{CO_3^{2-}} a_{CO_3^{2-}} + \nu_{Ca^{2+}}} \tag{4.8}$$

and

$$P_{CO_3^{2-}} = \frac{k_{CO_3^{2-}} a_{CO_3^{2-}} + \nu_{Ca^{2+}}}{k_{Ca^{2+}} a_{Ca^{2+}} + \nu_{CO_3^{2-}} + k_{CO_3^{2-}} a_{CO_3^{2-}} + \nu_{Ca^{2+}}}. \tag{4.9}$$

We modeled calcium isotope fractionation ($\Delta^{44/40}$Ca = 1000ln$\alpha_p \sim \delta^{44/40}Ca_{solid}$ - $\delta^{44/40}$Ca$_{fluid}$) corresponding to the range in calcium and carbonate activities obtained by mixing end-member lake and spring waters (Tables 4 & 5) using elementary exchange coefficients fitted to Larsen et al. (2010) obtuse step velocities, a fitted equilibrium fractionation factor of α_{eq} = 0.9996 and a fitted kinetic end-member fractionation factor of α_f = 0.9985. Attachment and detachment rate coefficients (k and ν values) and details of the fitting and calculation procedures may be found in Nielsen et al. (2012). Isotope fractionation as a function of solution stoichiometry of Mono Basin carbonate minerals is plotted in Fig. 8a, and modeled fractionation factors are compared with calculated values in Fig. 8b. The fractionation factor calculated for Mono Basin carbonates decreases with increasing $a_{Ca^{2+}}$:$a_{CO_3^{2-}}$, in agreement with the modeled trend.

As previously discussed, ion transport to the mineral surface cannot be the sole controlling factor determining the Ca isotope fractionation factor. Nevertheless, the slower diffusive transport of ^{44}Ca to the mineral surface could cause the surface aqueous ^{44}Ca/^{40}Ca to be lower than in bulk solution. This effect would tend to increase α_p, decreasing the magnitude of $\Delta^{44/40}$Ca, so that the full fractionation that would apply in a well-stirred fluid would not be observed. Overall, considering the likely uncertainties in our estimates of growth solution composition, the Mono Lake data conform to the model well. We tentatively conclude that the theoretically-predicted solution stoichiometry dependence of Ca isotope fractionation is in fact observed in this natural system. However, based on the fact that our calculated aragonite fractionation factors (-0.6 to -1.1 ‰; Table 6) are smaller than previously-measured experimental values (-1.4 to -1.8 ‰; Gussone et al., 2003, 2005), Mono Basin carbonate mineral growth may be partially diffusion-limited.

5. SUMMARY AND CONCLUSIONS

The Mono Lake carbonate cycle contrasts with the marine cycle in that it has high pH, low aqueous Ca concentration, and very low $a_{Ca^{2+}}$:$a_{CO_3^{2-}}$. We investigated the Ca isotope composition of Mono Lake waters, inflowing streams and springs, and precipitated carbonate minerals to determine whether the $a_{Ca^{2+}}$:$a_{CO_3^{2-}}$ ratio affects the Ca isotope fractionation during carbonate mineral precipitation. The carbonate system in Mono Lake, which is a closed basin lake, works much like the marine cycle in that the $\delta^{44/40}$Ca of the dissolved Ca in the lake is displaced to higher values relative to that of the dissolved Ca in streams supplying the lake, due to the influence of Ca isotope fractionation during removal of dissolved Ca by carbonate mineral precipitation. However, unlike the case for the global oceans, the residence time of Ca in Mono Lake is short, and the Ca isotopic composition of the lake water is subject to both spatial variability and relatively extreme temporal variations of $\delta^{44/40}$Ca.

The isotopic fractionation of Ca during precipitation, $\Delta^{44/40}$Ca$_C$, is estimated by comparing the $\delta^{44/40}$Ca of tufa and lake bottom sedimentary carbonate to the average $\delta^{44/40}$Ca of Mono Lake water. There is uncertainty associated with this comparison because the lake is a dynamic system that is subject to both natural variations and human disturbances, and the ages of tufa and lake bottom sediment samples are not known precisely. The residence time of Ca in the lake is only about 10 years, and there is spatial variation in the $\delta^{44/40}$Ca of Mono Lake water of about 0.4 ‰, and temporal variation of about 2.5 ‰. Nevertheless, we observe that the $\delta^{44/40}$Ca of carbonate minerals is consistently lower than that of the lake water by up to 1.75(21) ‰. This observation, combined with the observation that the lake water $\delta^{44/40}$Ca is higher than the average stream $\delta^{44/40}$Ca by about 1.1(2) ‰, indicates that the average value of $\Delta^{44/40}$Ca$_C$ for carbonate precipitation in Mono Lake must be about -1.1 ‰, which is consistent with the $\Delta^{44/40}$Ca$_{Tf}$ values calculated from mixing (Table 6). Diffusive Ca transport to the mineral-aqueous interface does not appear to be the primary control on Ca isotope incorporation into the bulk mineral, because the observed fractionation factors exceed the diffusive transport limit of $\sim$ -0.5 ‰.

The observed $\Delta^{44/40}$Ca for Mono Lake carbonates falls within the range of values observed in natural marine aragonite and inorganically precipitated carbonates at similar temperatures. Our results show that the magnitude of isotopic fractionation depends strongly on the ratio of Ca^{2+} to CO$_3^{2-}$ of the solution from which the carbonates grew. Carbonates precipitated near-shore from Ca-rich solutions have small $\Delta^{44/40}$Ca values, while carbonates that precipitated directly from high alkalinity, low-Ca lake water have larger $\Delta^{44/40}$Ca values. The observed relationship between calcium isotope fractionation and solution stoichiometry can be explained using the theory developed in Nielsen et al. (2012).

Our results confirm that Ca isotope fractionation during precipitation of carbonate minerals from aqueous solution is controlled by the kinetics of ion attachment and detachment fluxes at the mineral aqueous interface and depends on the $a_{Ca^{2+}}$:$a_{CO_3^{2-}}$ ratio. Because kinetic processes affect isotopic and trace element incorporation into precipitated carbonate minerals, using Ca isotopes to reconstruct paleo-seawater isotopic composition (e.g. Farkaš et al., 2007; Fantle and DePaolo, 2007) in general requires knowledge of precipitation rate, the stoichiometry of the growth solution and potentially other factors as well. This clearly complicates the application of isotopes for seawater reconstruction, but also may mean that Ca isotopes may provide information on paleo-seawater composition. Non-equilibrium effects (i.e. kinetic or vital effects) are also important and must be accounted for in paleo-environmental reconstructions with C and O isotopes (e.g. Zachos et al., 2001). Understanding the controls on Ca isotope fractionation may bring new insights about kinetic processes controlling the isotopic composition of carbonate minerals, which could be useful in the interpretation of the C and O isotopic systems.

REFERENCES

Bertram M.A., Mackenzie F.T., Bishop F.C., and Bischoff W.D. (1991) Influence of temperature on the stability of magnesian calcite. *Am. Mineral.* **76**, pp. 1889–1896.

Bischoff J.L., Stine S., Rosenbauer R.J., Fitzpatrick J.A., and Stafford T.W. (1993) Ikaite precipitation by mixing of shoreline springs and lake water, Mono Lake, California, USA. *Geochim. Cosmochim. Acta* **57**(16), pp. 3855–3865.

Bischoff W.D., Mackenzie F.T., and Bishop F.C. (1987) Stabilities of synthetic magnesian calcites in aqueous solution: comparison with biogenic materials. *Geochim. Cosmochim. Acta* **51**, pp. 1413–1423.

Blum J.D., Erel Y., and Brown K. (1993) ^{87}Sr/^{86}Sr ratios of Sierra Nevada stream waters: Implications for relative mineral weathering rates. *Geochim. Cosmochim. Acta* **58**, pp. 5019–5025.

Böhm F., Gussone N., Eisenhauer A., Dullo W.C., Reynaud S., and Paytan A. (2006) Calcium isotope fractionation in modern scleractinian corals. *Geochim. Cosmochim. Acta* **70**(17), pp. 4452–4462.

Bourg I.C. and Sposito G. (2007) Molecular dynamics simulations of kinetic isotope fractionation during the diffusino of ionic species in liquid water. *Geochim. Cosmochim. Acta* **71**, pp. 5583–5589.

Bourg I.C., Richter F.M., Christensen J.N., and Sposito G. (2010) Isotopic mass-dependence of metal cation diffusion coefficients in liquid water. *Geochim. Cosmochim. Acta* **74**, pp. 2249–2256.

Burton E.A. and Walter L.M. (1990) The role of pH in phosphate inhibition of calcite and aragonite precipitation rates in seawater. *Geochim. Cosmochim. Acta* **54**, pp. 797–808.

Chang V.T.C., Williams R.J.P., Makishima A., Belshawl N.S., and O'Nions R.K. (2004) Mg and Ca isotope fractionation during $CaCO_3$ biomineralisation. *Biochem. Bioph. Res. Co.* **323**(1), pp. 79–85.

Cloud P. and LaJoie K.R. (1980) Calcite-impregnated defluidization structures in littoral sands of Mono Lake, California. *Science* **210**, pp. 1009–1012.

DePaolo D. (2011) Surface kinetic model for isotopic and trace element fractionation during precipitation of calcite from aqueous solutions. *Geochim. Cosmochim. Acta* **75**(4), pp. 1039–1056.

DePaolo D.J. (2004) Calcium isotopic variations produced by biological, kinetic, radiogenic and nucleosynthetic processes. *Geochemistry of non-traditional stable isotopes* (eds. C.M. Johnson, B.L. Beard, and F. Albarede), Rev. Mineral. Geochem., volume 56, pp. 255–285.

Dietzel M., Tang J., Leis A., and Koehler S.J. (2009) Oxygen isotopic fractionation during inorganic calcite precipitation - Effects of temperature, precipitation rate and pH. *Chem. Geol.* **268**(1-2), pp. 107–115.

Dove P.M. and Hochella M.F. (1993) Calcite precipitation mechanisms and inhibition by orthophosphate - In situ observations by scanning force microscopy. *Geochim. Cosmochim. Acta* **57**(3), pp. 705–714.

Dunn J.R. (1953) Origin of the deposits of tufa in Mono Lake. *J. Sediment. Petrol.* **23**(1), pp. 18–23.

EIR (1993) *California State Wat. Res. Control Board, Mono Basin Environmental Impact Report* .

Fantle M.S. and DePaolo D.J. (2005) Variations in the marine Ca cycle over the past 20 million years. *Earth Planet. Sci. Lett.* **237**, pp. 102–117.

Fantle M.S. and DePaolo D.J. (2006) Sr isotopes and pore fluid chemistry in carbonate sediment of the Ontong Java Plateau: Calcite recrystallization rates and evidence for a rapid rise in seawater Mg over the last 10 million years. *Geochim Cosmochim Acta* **70**, pp. 3883–3904.

Fantle M.S. and DePaolo D.J. (2007) Ca isotopes in carbonate sediment and pore fluid from ODP Site 807A: The Ca2+(aq)-calcite equilibrium fractionation factor and calcite recrystallization rates in Pleistocene sediments. *Geochim. Cosmochim. Acta* **71**(10), pp. 2524–2546.

Farkaš J., Böhm F., Wallmann K., Blenkinsop J., Eisenhauer A., van Geldern R., Munnecke A., Voight S., and Veizer J. (2007) Calcium isotope record of Phanerozoic oceans: Implications for chemical evolution of seawater and its causative mechanisms. *Geochim. Cosmochim. Acta* **71**, pp. 5117–5134.

Garrels R.M. and Mackenzie F.T. (1967) Origin of chemical compositions of some springs and lakes. *Adv. Chem. Ser.* **67**, p. 222.

Gussone N., Eisenhauer A., Heuser A., Dietzel M., Bock B., Böhm F., Spero H.J., Lea D.W., Bijma J., and Nägler T.F. (2003) Model for kinetic effects on calcium isotope fractionation (δ^{44}Ca) in inorganic aragonite and cultured planktonic foraminifera. *Geochim. Cosmochim. Acta* **67**(7), pp. 1375–1382.

Gussone N., Langer G., Geisen M., Eisenhauer A., and Riebesell U. (2004) Ca isotope fractionation in coccolithophores. *Geochim. Cosmochim. Acta* **68**(11), pp. A207–A207.

Gussone N., Böhm F., Eisenhauer A., Dietzel M., Heuser A., Teichert B.M.A., Reitner J., Worheide G., and Dullo W.C. (2005) Calcium isotope fractionation in calcite and aragonite. *Geochim. Cosmochim. Acta* **69**(18), pp. 4485–4494.

Gussone N., Nehrke G., and Teichert B.M. (2011) Calcium isotope fractionation in ikaite and vaterite. *Chem. Geol.* **285**, pp. 194–202.

Heuser A. and Eisenhauer A. (2008) The calcium isotope composition ($\delta^{44/40}$Ca) of NIST SRM 915b and NIST SRM 1486. *Geostand. Geoanal. Res.* **32**, pp. 311–315.

Horwitz E.P., McAlister D.R., Bond A.H., and Barrans R.E. (2005) Novel extraction of chromatographic resins based on tetraalkyldiglycolamides: Characterization and potential applications. *Solvent Extr. Ion Exch.* **23**(3), pp. 319–344.

Jellison R. and Roll S. (2003) Weakening and near breakdown of meromixis in Mono Lake

.

Jellison R., Macintyre S., and Millero F. (1993a) Density and conductivity properties of Na-CO_3-Cl-SO_4 brines from Mono Lake, California, USA. *Int. J. Salt Lake Res.* **8**, pp. 41–53.

Jellison R., Miller L.G., Melack J.M., and Dana G.L. (1993b) Meromixis in hypersaline Mono Lake, California. 2. Nitrogen fluxes. *Limnol. Oceanogr.* **38**(5), pp. 1020–1039.

Johnson C., Beard B., Roden E., Newman D.K., and Nealson K.H. (2004) Isotopic constraints on biogeochemical cycling of Fe. *Rev. Mineral. Geochem.* **55**(1), pp. 359–408.

Kim S. and O'Neil J.R. (1997) Equilibrium and nonequilibrium oxygen isotope effects in synthetic carbonates. *Geochim. Cosmochim. Acta* **61**(16), pp. 3461–3475.

LADWP L.A.D.W.P. (2010) *Aqueduct Northern District Daily Report*, p. Also available at at http://www.ladwp.com/ladwp/cms/ladwp005341.jsp.

Larsen K., Bechgaard K., and Stipp S.L.S. (2010) Modelling spiral growth at dislocations and determination of critical step lengths from pyramid geometries on calcite surfaces. *Geochim. Cosmochim. Acta* **74**(2), pp. 558–567.

Lemarchand D., Wasserburg G., and Papanastassiou D.A. (2004) Rate-controlled calcium isotope fractionation in synthetic calcite. *Geochim. Cosmochim. Acta* **68**(22), pp. 4665–4678.

Li H.C. (1995) *Isotope geochemistry of Mono Basin, California: applications to paleoclimate and paleohydrology*. Ph.D. thesis, University of Southern California.

Lin Y. and Singer P.C. (2006) Inhibition of calcite precipitation by orthophosphate: Speciation and thermodynamic considerations. *Geochim. Cosmochim. Acta* **70**, pp. 2530–2539.

Morse J.W. and Arvidson R.S. (2002) The dissolution kinetics of major sedimentary carbonate minerals. *Earth-Sci. Rev.* **58**(1-2), pp. 51–84.

Morse J.W., Arvidson R.S., and Lüttge A. (2007) Calcium carbonate formation and dissolution. *Chem. Rev.* **107**, pp. 342–381.

Neumann K. and Dreiss S. (1995) Strontium 87/strontium 86 ratios as tracers in groundwater and surface waters in Mono Basin, California. *Water Resour. Res.* **31**(12), pp. 3183–3193.

Newton M. (1994) Holocene fluctuations of Mono Lake, California: the sedimentary record. *Sedimentology and Geochemistry of Modern and Ancient Saline Lakes* (eds. R.W. Renaut and W.M. Last), Society for Sedimentary Geology, Tulsa, pp. 143–158.

Nielsen L.C., Druhan J.L., Yang W., Brown S.T., and DePaolo D.J. (2011) Calcium isotopes as tracers of biogeochemical processes. *Handbook of Environmental Isotope Geochemistry* (ed. M. Baskaran), Springer, New York, volume 1, chapter 7, pp. 105–124.

Nielsen L.C., DePaolo D.J., and Yoreo J.J.D. (2012) Self-consistent ion-by-ion growth model for kinetic isotope fractionation during calcite precipitation. *Geochim. Cosmochim. Acta* .

Reynard L.M., Day C.C., and Henderson G.M. (2011) Large fractionation of calcium isotopes during cave-analogue calcium carbonate growth. *Geochim. Cosmochim. Acta* **75**, pp. 3726–3740.

Richter F.M., Mendybaev R.A., Christensen J.N., Hutcheon I.D., Williams R.W., Sturchio N.C., and Beloso A.D. (2006) Kinetic isotopic fractionation during diffusion of ionic species in water. *Geochim. Cosmochim. Acta* **70**(2), pp. 277–289.

Rocha C.D.L. and DePaolo D.J. (2000) Evidence for variations in marine calcium cycle over the Cenozoic. *Science* **289**, pp. 1176–1178.

Russell I.C. (1889) Quaternary History of Mono Valley, California. *Eighth Annual Report of the USGS*, pp. 267–394.

Scholl D. and Taft W. (1964) Algae, contributors to the formation of calcareous tufa, Mono Lake, California. *J. Sediment. Res.* **34**(2), pp. 309–319.

Simon J.I. and DePaolo D.J. (2010) Stable calcium isotopic composition of meteorites and rocky planets. *Earth Planet. Sci. Lett.* **289**(3-4), pp. 457–466.

Skulan J. and DePaolo D.J. (1999) Calcium isotope fractionation between soft and mineralized tissues as a monitor of calcium use in vertebrates. *Proc. Natl. Acad. Sci.* .

Steefel C.I. (2009) CrunchFlow: Software for modeling multicomponent reactive flow and transport. *Users Manual* .

Tang J., Dietzel M., Böhm F., Kohler S., and Eisenhauer A. (2008) Sr^{2+}/Ca^{2+} and $^{44}Ca/^{40}Ca$ fractionation during inorganic calcite formation: II. Ca isotopes. *Geochim. Cosmochim. Acta* **72**, pp. 3733–3745.

Tomascak P.B., Hemming G.N., and Hemming S.R. (2003) The lithium isotopic composition of waters of the Mono Basin, California. *Geochim. Cosmochim. Acta* **67**(4), pp. 601–611.

Whiticar M.J. and Suess E. (1998) The cold carbonate connection between Mono Lake, California and the Bransfield Strait, Antarctica. *Aquatic Geochem.* **4**, pp. 429–454.

Zachos J., Pagani M., Sloan L., Thomas E., and Billups K. (2001) Trends, rhythms, and aberrations in global climate 65 Ma to present. *Science* **292**, pp. 686–693.

LIST OF TABLES

Table 1: Stoichiometry and solubility data for the high and low magnesian calcite added to the CrunchFlow(2007) thermodynamic database for this study. The stoichiometric coefficient of magnesium for each of the magnesian calcite phases is listed under X.

Species	**X**	**-log(K_{sp})**	**Molecular Mass**
High Mg Calcite	0.15	8.40 (Bischoff et al., 1987)	97.7209
Low Mg Calcite	0.07	8.48 (Bertram et al., 1991)	98.9828

Table 2: Mineralogy of solid samples collected along the northern shore of Mono Lake, determined via x-ray diffraction. Most tufa samples are primarily aragonite with lesser magnesian calcite, calcite, quartz and evaporite minerals. Minerals are listed in order of decreasing abundance.

Sample	**Easting (m)**	**Northing (m)**	**Type**	**Mineralogy**
Crust 1	317300	4210496	Salt crust	Trona, Burkeite
Crust 3	318663	4212644	Salt crust	Calcite, Aragonite, Quartz, Halite
Tufa 1	317300	4210496	Tufa	Aragonite, Magnesian Calcite, Quartz
Tufa 2	317389	4210453	Tufa	Aragonite, Magnesian Calcite, Quartz
Tufa 3	317478	4210568	Tufa	Aragonite, Magnesian Calcite, Quartz
Tufa 4	317543	4210716	Tufa	Aragonite
Tufa 5	318705	4212994	Tufa	Aragonite, Halite
Tufa 6	318674	4212785	Tufa	Aragonite, Trona, Burkeite
Tufa 7	318714	4212789	Tufa	Aragonite
Tufa 8	318675	4212657	Tufa	Aragonite, Burkeite
Tufa 9	321800	4214941	Tufa	Magnesian Calcite, Halite
Tufa 10	321900	4214934	Tufa	Aragonite, Trona, Quartz, Calcite
LBS 1			Sediment	Quartz, Aragonite, Halite, Muscovite, Anorthite
LBS 2	323202	4203334	Sediment	Quartz, Albite, Calcite, Microcline, Aragonite
LBS 3	325380	4215900	Sediment	Quartz, Albite, Halite, Magnesian Calcite, Aragonite

Table 3: Calcium and strontium isotopic composition and concentration analyses of water and solid samples from the Mono Basin. Uncertainties for ^{87}Sr/^{86}Sr are reported when they exceed 1e-5. Abbreviation "FW" stands for freshwater, "LBS" for lake bottom sediment, and "UN" for unnamed. Mono Lake water samples Lk. 2009 9-12 are a depth profile of the lake at 3, 10, 15 and 17.5 m (lake bottom). Ca isotopic compositions are averaged from duplicate analyses on all samples. Concentrations of Sr and Ca have an uncertainty of ± 2%. Samples are classified according to 8 types: depleted spring (DS), spring (Sp), Mono Lake water (ML), Northern freshwater (NF), shoreline crust (CR), tufa tower (TF), lake bottom sediment (LBS), and Sierra Nevada stream (SNS). Archived samples are denoted by *.

Sample	**Type**	$\delta^{44/40}$**Ca (‰ BSE)**	**[Ca] (ppm)**	^{87}**Sr/**^{86}**Sr**	**[Sr] (ppm)**	**[Sr]/[Ca] (×** $\mathbf{10^3}$**)**
Spring 1	DS	0.45	1.61	0.70847	7.59e-3	4.71
Spring 2 FW	DS	0.34	1.21	0.70841	1.52e-3	1.26
Spring 3	DS	0.78	2.06	0.70814(9)	7.96e-3	3.86
Waford Sp.*	SP	-0.36	1.62	0.70750	1.17e-2	7.23
Indian Sp.*	SP	-0.38	18.5	0.70646	2.31e-1	12.5
Tufa Sp.*	SP	-0.80	23.7	0.70971	8.13e-2	3.47
FOY Sp.*	SP	-0.74	20.3	0.70976	7.22e-2	3.56
Cow Sp.*	SP	-0.83	4.71	0.70640	4.89e-2	1.04
Lk. 1996*	ML	2.14	2.54	-	-	-
Lk. 2004-1*	ML	-0.07	12.9	-	-	-
Lk. 2004-2*	ML	-0.27	12.0	-	-	-
Lk. 2005*	ML	0.80	4.24	0.70917	3.20e-2	7.55
Lk. 2009-1	ML	0.48	7.37	-	-	-
Lk. 2009-2	ML	0.25	7.66	0.70908(3)	1.27e-2	1.66
Lk. 2009-6	ML	0.60	7.09	0.70912(2)	2.11e-2	2.97
Lk. 2009-8	ML	0.43	7.77	0.7089(1)	2.94e-2	3.78
Lk. 2009-9	ML	0.16	8.10	0.70916(6)	3.15e-2	3.88
Lk. 2009-10	ML	0.33	8.09	0.70914	3.13e-2	3.87
Lk. 2009-11	ML	0.31	7.95	-	3.15e-2	3.96
Lk. 2009-12	ML	0.16	7.82	0.70902(4)	3.17e-2	4.05
Lk. 2010	ML	0.26	8.34	0.70896	2.98e-2	3.58
Freshwat. Lk	NF	-0.19	10.9	0.70825	8.21e-2	7.55
Wilson Ck	NF	-0.44	8.41	0.70971	2.51e-2	2.99

Continued on Next Page…

Sample	**Type**	$\delta^{44/40}$**Ca (‰ BSE)**	**[Ca] (ppm)**	^{87}**Sr/**^{86}**Sr**	**[Sr] (ppm)**	**[Sr]/[Ca] (× 10**^{3}**)**
Crust 1	CR	-0.70	3.01e3	0.70853	1.97e1	6.55
Crust 3	CR	-0.57	1.09e5	0.70876	6.91e2	6.32
Tufa 1	TF	-0.40	2.89e5	0.70891	2.42e3	7.36
Tufa 2	TF	-0.73	3.46e5	0.70893	2.13e3	6.15
Tufa 3	TF	-0.71	3.46e5	0.70895	1.99e3	5.76
Tufa 4	TF	-0.65	3.88e5	0.70900	2.62e3	7.38
Tufa 5	TF	-0.56	3.66e5	0.70902	2.20e3	6.02
Tufa 6	TF	-0.55	1.45e5	0.70898	8.00e2	5.53
Tufa 8	TF	-0.68	1.72e5	0.70893	7.77e2	4.52
Tufa 10	TF	-0.69	3.39e5	0.70899	2.09e3	6.17
Tufa 11	TF	-0.64	3.25e5	0.70899	1.91e3	5.87
LBS 1	LBS	-0.30	-	0.70904	-	-
LBS 2	LBS	-0.39	-	0.70905	-	-
LBS 3	LBS	-0.78	-	0.70883	-	-
LBS 4	LBS	-0.94	-	0.70889	-	-
Lee Vining Ck.	SNS	-0.68	3.97	0.70976	1.50e-2	3.78
Rush Ck.	SNS	-0.83	6.02	0.70971	1.89e-2	3.15
UN Ck. 1	SNS	-0.79	12.8	0.71153	3.40e-2	2.66
UN Ck. 2	SNS	-0.77	5.95	0.70882	4.66e-2	7.83

Table 4: Concentrations of major dissolved constituents of Mono Basin fluids. Lake water composition reported here was sampled in the summer of 2010 at the same location as LBS 2 listed above.

	Mono Lake (ppm)	**High-Ca Spring**[a] (ppm)
T (°C)	18.9	15
pH	9.8	6.5
Na	27300	132
K	1460	12
Ca[b]	4.24	23
Mg	37	37
Alkalinity[c]	30400	845
Cl	17300	44
SO_4	9880	36
SiO_2	16	81
PO_3	51	0

(a) Spring water composition from Bischoff et al. (1993) Table 1, Spring 3.
(b) Calcium concentration of lake water is assumed to be the steady state value. Spring water is assumed to have the same concentration as Tufa spring.
(c) Alkalinity as ppm HCO_3.

Table 5: End-member spring and lake water isotopic compositions used to calculate the proportion of lake and spring water in solutions from which tufa precipitated. Steady state lake water was assumed to have an isotopic composition equal to the value measured in lake water with $\sim$ 4 ppm Ca. End-member spring water was assumed to have a calcium concentration and isotopic composition identical to Tufa spring, and a strontium isotopic composition similar to northern spring water.

	[Ca] (ppm)	**[Sr]** (ppm)	$\delta^{44/40}$**Ca** (‰ BSE)	^{87}**Sr/**^{86}**Sr**
Lake water	4.20	0.032	0.80	0.70908(21)
Spring water	23.7	0.081	-0.80	0.70834(35)

Table 6: Ca isotope fractionation for a given solution stoichiometry during Mono Basin carbonate growth from mixed spring-lake water, using end-member compositions listed in Table 5. $\Delta^{44/40}$Ca values calculated assuming a lake water calcium isotopic composition equal to the 2009 average value (0.34(14)) and assuming a lake water calcium isotopic composition equal to the 1996 value (2.14) were also calculated and are the first and second values respectively listed in parentheses. Propagation of uncertainty for the isotopic compositions of the end-member fluids and carbonate minerals (0.15) yields an overall uncertainty for each $\Delta^{44/40}$Ca of 0.21 ‰.

Sample	**Fraction lake water**[a] (x)	**2 s.d.**	$a_{Ca^{2+}} : a_{CO_3^{2-}}$	**2 s.d.**	$\Delta^{44/40}$**Ca** [b] (‰)
Crust 1	0.47	0.03	1.3	0.1	-0.12 (-0.06, -0.31)
Crust 3	0.78	0.01	0.27	0.03	-0.38 (-0.20, -0.88)
Tufa 1	0.90	0.04	0.074	0.04	-0.56 (-0.29, -1.37)
Tufa 2	0.92	0.03	0.053	0.02	-0.98 (-0.67, -1.83)
Tufa 3	0.93	0.01	0.044	0.01	-1.01 (-0.69, -1.91)
Tufa 4	0.96	0.01	0.021	0.01	-1.11 (-0.75, -2.17)
Tufa 5	0.97	0.02	0.015	0.01	-1.09 (-0.72, -2.21)
Tufa 6	0.95	0.02	0.028	0.01	-0.96 (-0.61, -1.97)
Tufa 8	0.91	0.01	0.055	0.01	-0.92 (-0.63, -1.79)
Tufa 10	0.95	0.01	0.024	0.01	-1.13 (-0.78, -2.18)
Tufa 11	0.95	0.02	0.024	0.010	-1.08 (-0.73, -2.12)
LBS 1	1.00	0.003	0.001	0.001	-1.10 (-0.64, -2.44)
LBS 2	1.00	0.005	0.001	0.001	-1.20 (-0.74, -2.54)
LBS 3	0.84	0.01	0.16	0.004	-0.74 (-0.53, -1.38)
LBS 4	1.00	0.002	0.001	0.001	-1.75 (-1.29, -3.09)

(a) Calculated from the intersection of solid ^{87}Sr/^{86}Sr and the spring-Mono Lake water mixing line (Fig. 6).
(b) Calculated by difference between $\delta^{44/40}$Ca of solid and mixed water for a given strontium isotopic composition (Fig. 7).

LIST OF FIGURES

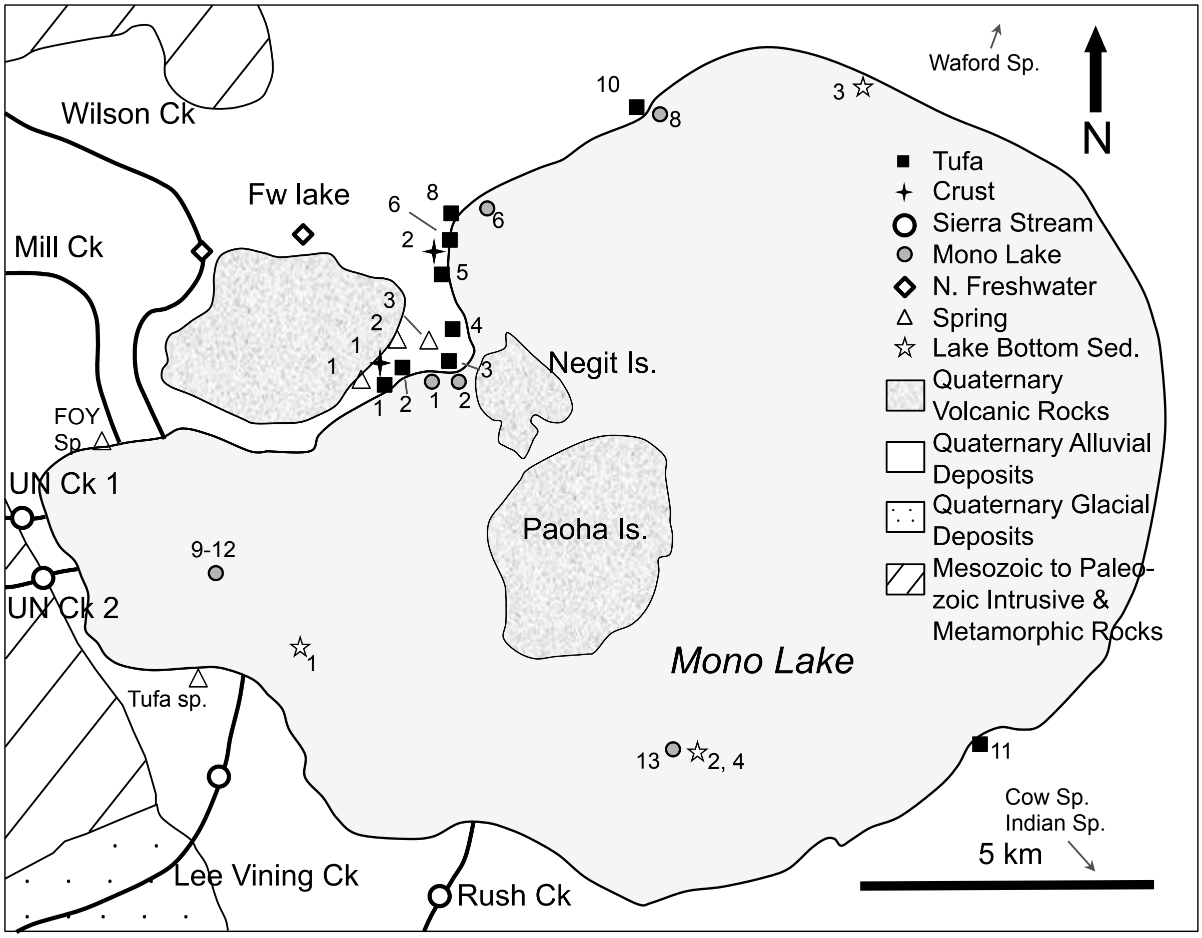

Figure 1: Map of sampling locations in the Mono Basin (geology based on Tomascak et al. (2003)). Strontium isotopic compositions of spring and stream waters vary significantly with location due to the effects of underlying lithology (Table 3). Details of solid sample position and mineralogy can be found in Table 2. The location of the freshwater lake is indicated by an open diamond labeled “Fw lake.” Northern depleted springs referred to in the text include springs (open triangles) labeled 1, 2 and 3. Abbreviations “Ck,” “Is,” “Fw,” and “Sp.” refer to creek, island, freshwater, and spring respectively.

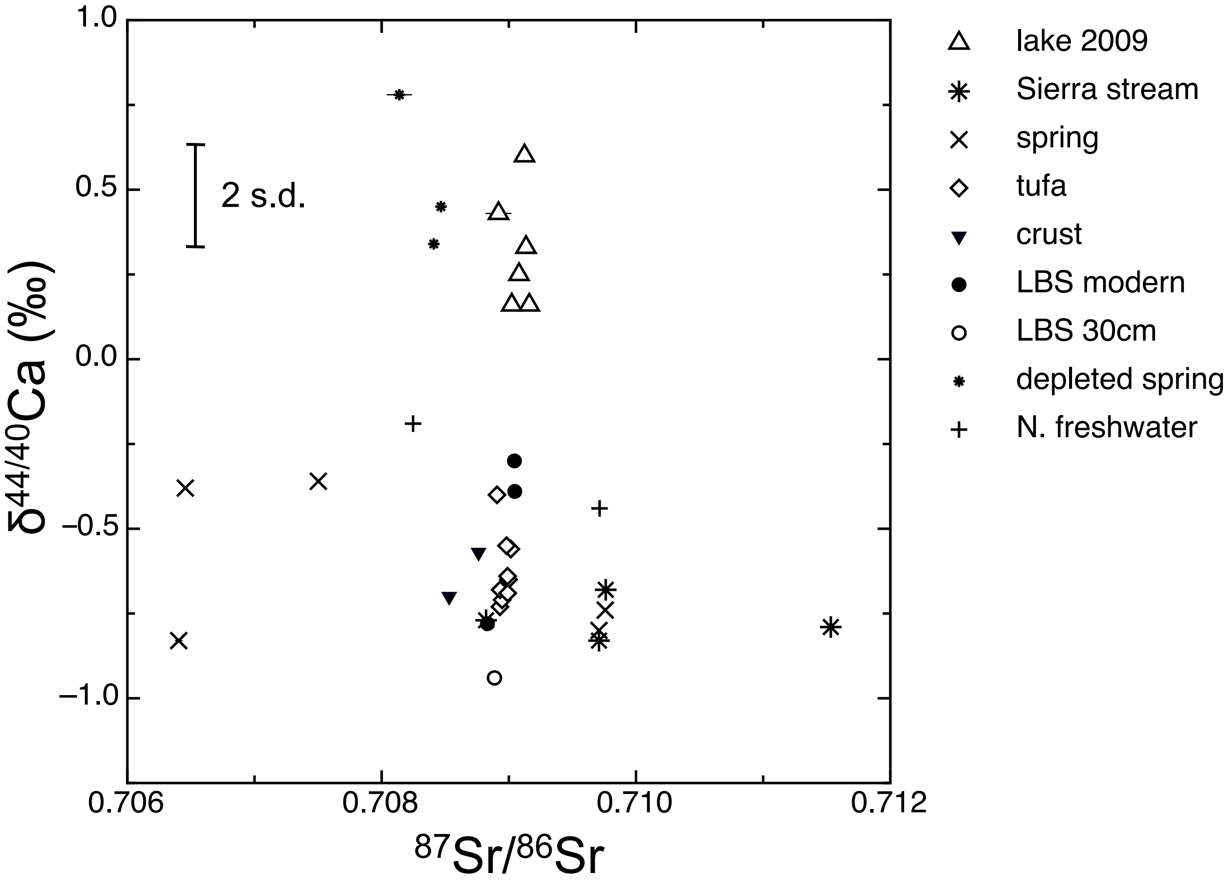

Figure 2: Sr and Ca (BSE) isotopic compositions of Mono Basin samples. Standard errors for ^{87}Sr/^{86}Sr are marked for each sample and are smaller than marker size if not visible. The label LBS represents lake bottom sediment.

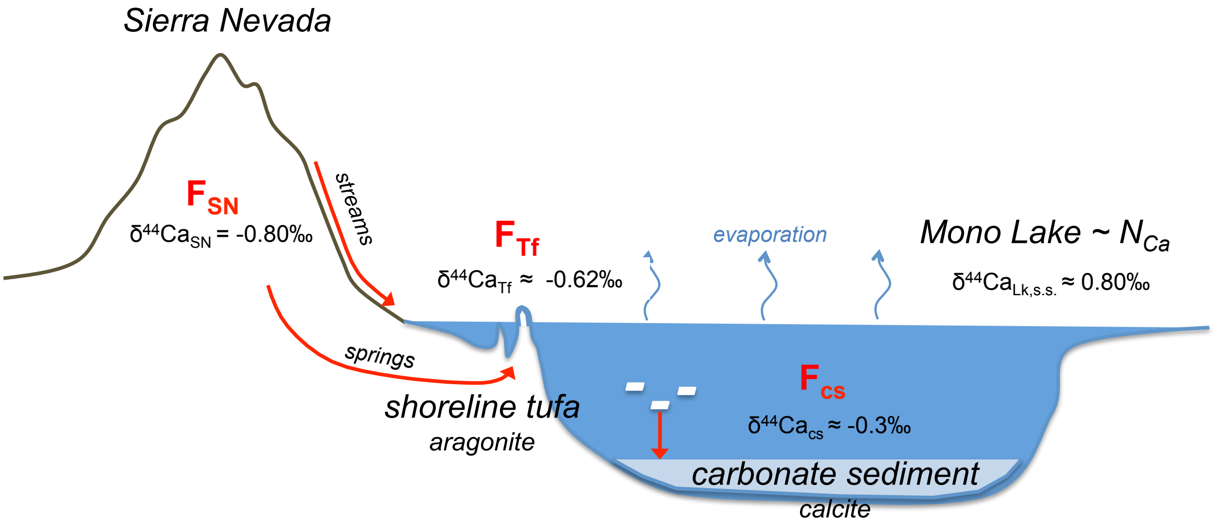

Figure 3: Ca budget for Mono Basin. The primary Ca flux into Mono Lake (F_{SN}) results from chemical weathering of minerals in the Sierra Nevada, with a low average $\delta^{44/40}$Ca. The primary flux of Ca out of Mono Lake is via calcareous tufa precipitation (F_{Tf}) and flux of carbonate to lake bottom sediment (F_{cs}). Total moles of dissolved Ca in Mono Lake are N_{Ca}, and the Ca isotope fractionation during tufa precipitation is $\Delta^{44/40}Ca_{Tf}$.

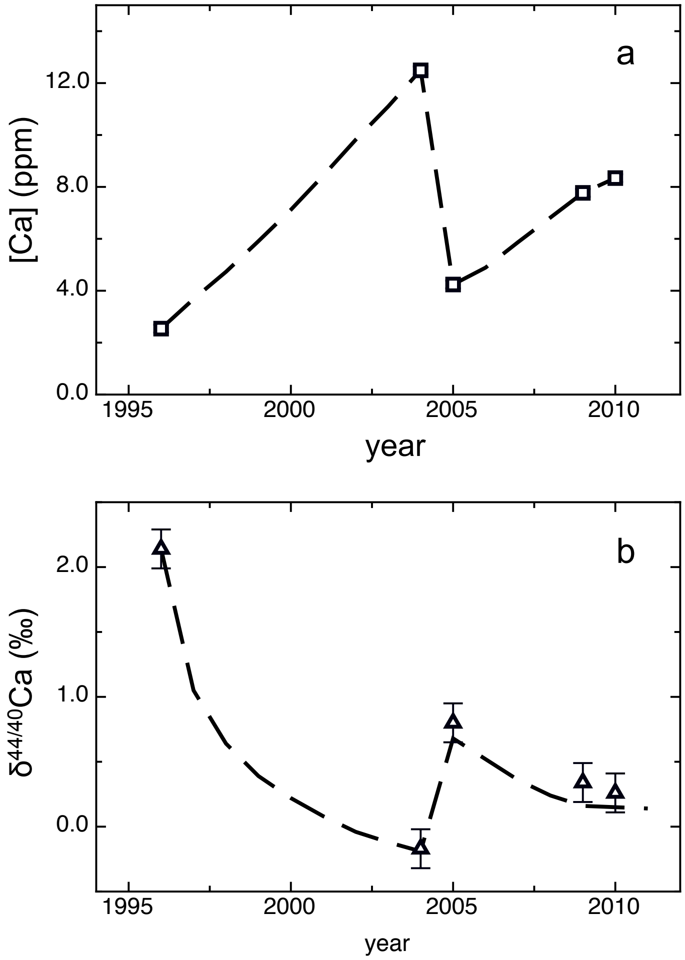

Figure 4: a) Calcium concentrations and b) isotopic compositions of Mono Lake water analyzed in this study. The dashed line in both figures represents the fitted Mono Lake calcium budget based on Eq. 4.1. The abrupt decrease in calcium concentration between 2004-2005 coincides with the breakdown of meromixis recorded in 2003.

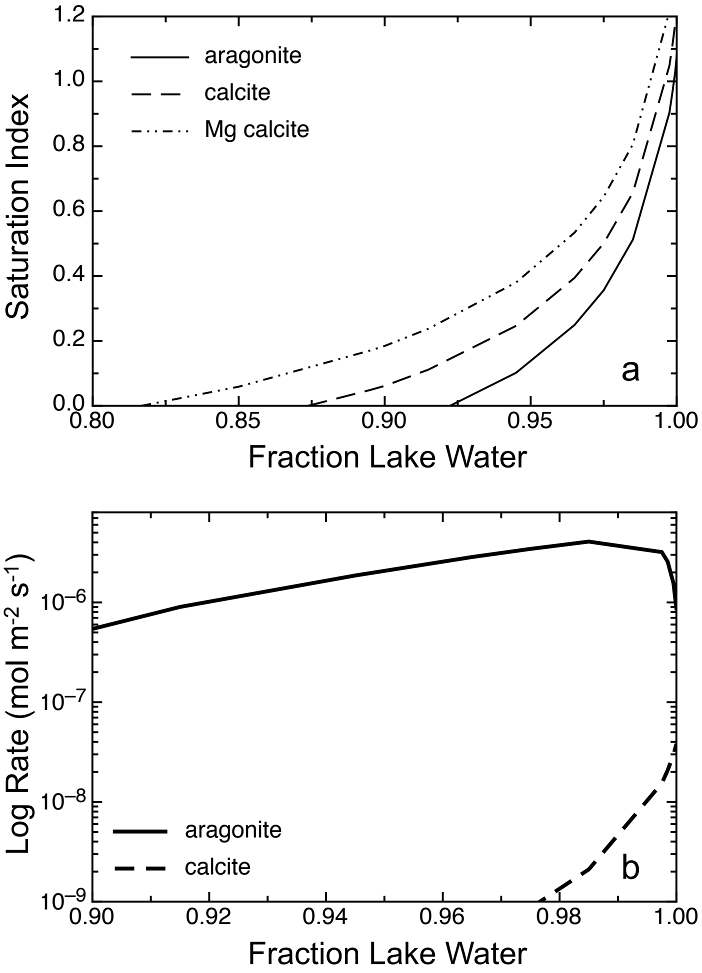

Figure 5: a) Saturation index with increasing lake water fraction during mixing with Ca-rich spring water. Saturation index increases monotonically with % lake water, but observations indicate precipitation occurs during mixing of Mono Lake and spring water. b) Precipitation rate calculated as a function of fraction lake water during mixing with typical high-Ca shoreline spring water. Spring water composition is based on Bischoff et al. (1993) with a calcium concentration equal to Tufa spring. Spring water addition negates the effects of phosphate inhibition on pure Mono Lake water.

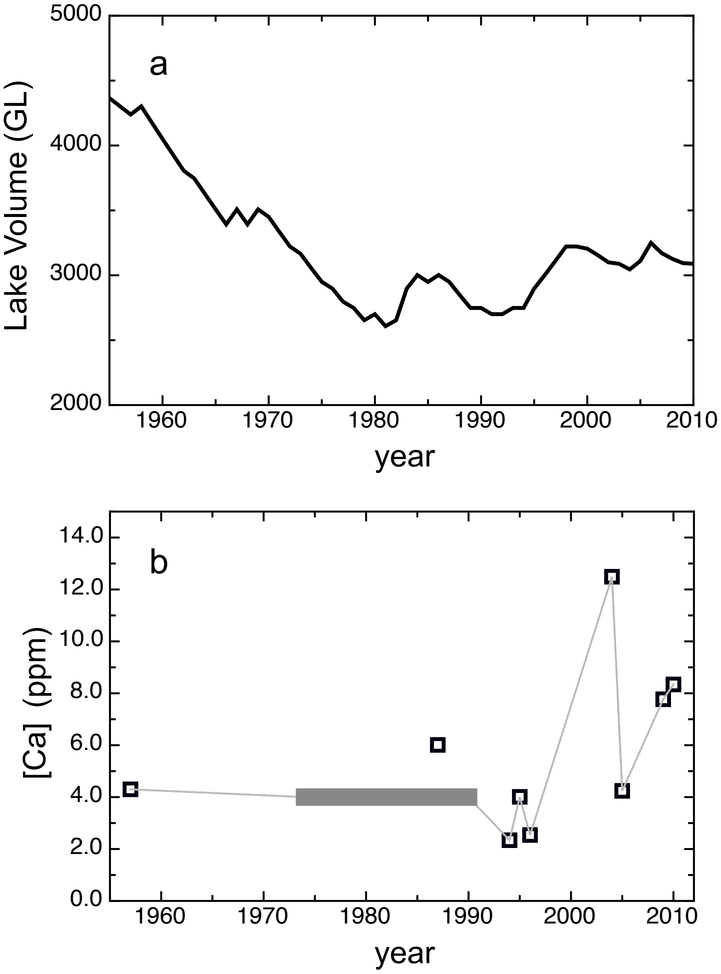

Figure 6: a) Mono Lake volume in billions of liters (GL) and b) calcium concentration between 1955 and 2010. Lake volume decreased dramatically between 1940 until 1980 due to stream water diversions by the LADWP. The calcium concentration of Mono Lake water had a median value of 4 ppm between 1974 and 1990 (EIR, 1993), represented by the solid gray bar.

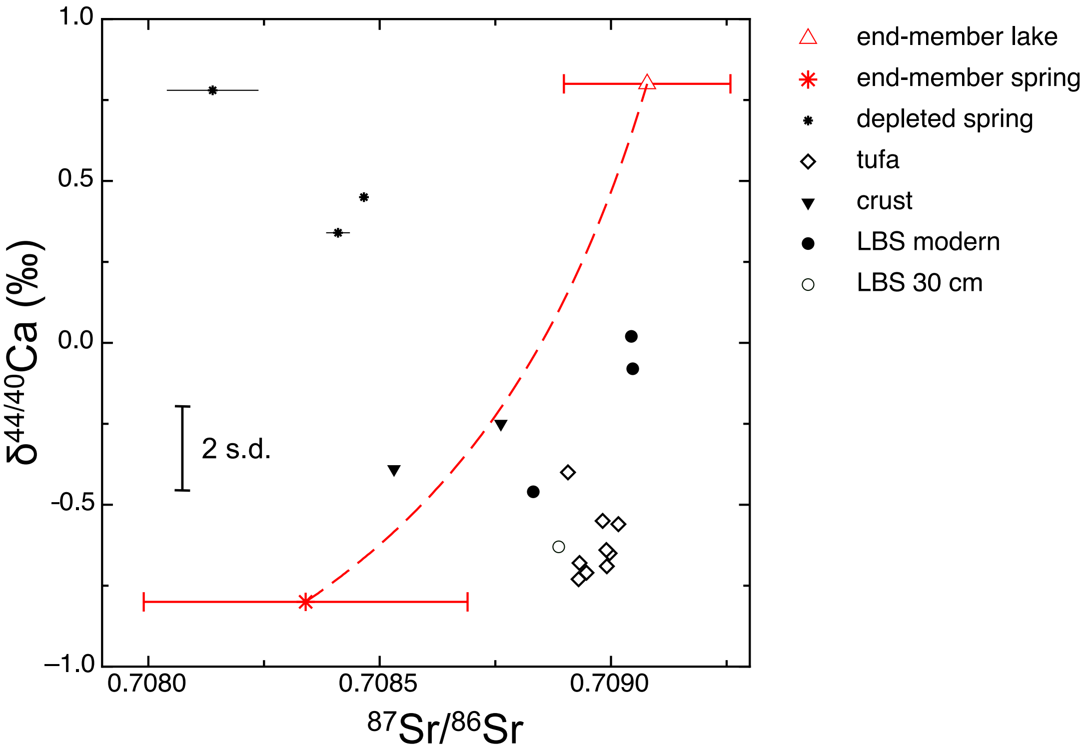

Figure 7: Detail of spring-lake water mixing to produce solid tufa carbonates and crusts. End-member lake water has an average Sr isotopic composition of all lake waters analyzed (1996-2010), and the Ca isotopic composition of 4 ppm lake water (2005), which is thought to represent the long term average composition. End-member spring water has an average Sr isotopic composition of depleted springs, which were sampled adjacent to tufa and therefore has an isotopic composition representative of local spring water. The Ca isotopic composition and concentration of Tufa spring, the highest Ca spring water analyzed, was assigned to the end-member spring water composition. Fractionation factors of tufa and crusts were calculated by subtracting the mixed isotopic composition at the appropriate ^{87}Sr/^{86}Sr from the measured solid $\delta^{44/40}$Ca.

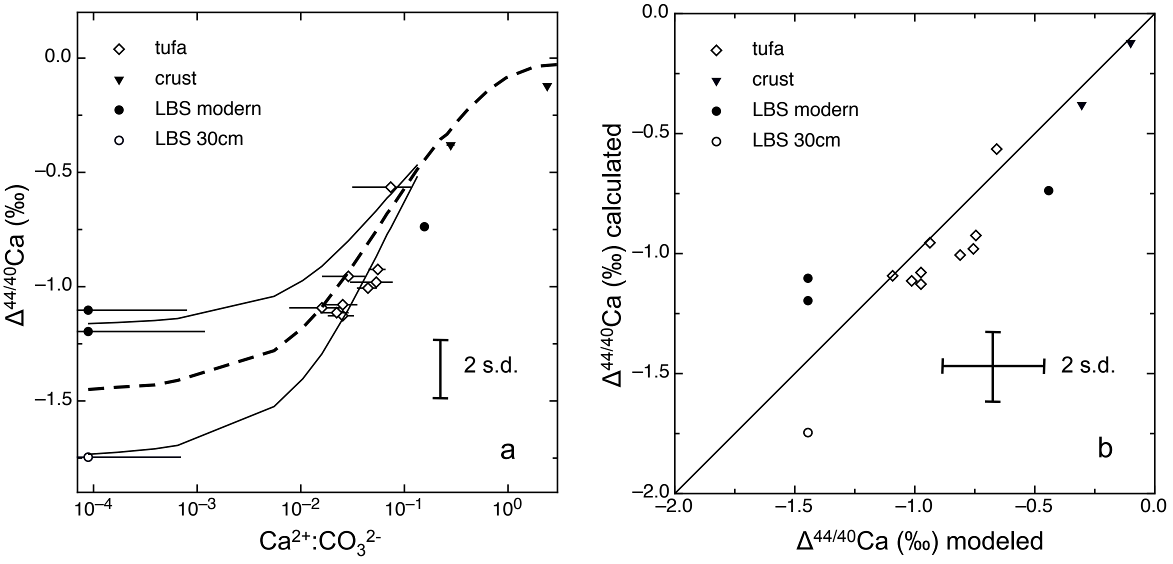

Figure 8: a) Model fit to Mono carbonate $\Delta^{44/40}$Ca calculated from Eq. 4.7 using $k_{Ca^{2+}}$, $k_{CO_3^{2-}}$, $\nu_{Ca^{2+}}$, and $\nu_{CO_3^{2-}}$ fitted to Larsen et al. (2010) step velocities in Nielsen et al. (2012). Activities of calcium and carbonate were calculated based on mixing of end-member spring and lake water compositions (Table 5) at varied proportions. The $a_{Ca^{2+}}$:$a_{CO_3^{2-}}$ dependence of Ca isotope fractionation of carbonate precipitation assuming a -0.4 ‰ equilibrium $\Delta^{44/40}$Ca and -1.5 ‰ (dashed line), -1.2 ‰ (top solid line) and -1.8 ‰ (bottom solid line) kinetic end-member $\Delta^{44/40}$Ca values. Solution stoichiometry for each sample was determined from the fraction lake water extracted from the Sr-Ca mixing line (Figure 4). “LBS modern” and “LBS 30 cm” were taken from the same core and correspond to samples LBS 2 and LBS 4 in Table 3. b) Modeled vs. calculated fractionation factor during precipitation corresponding to the -1.5 ‰ kinetic end-member fractionation factor, with the 1:1 line drawn to guide the eye.